Scripta Materialia 186 (2020) 185–189

Contents lists available at ScienceDirect

Scripta Materialia

journal homepage: www.elsevier.com/locate/scriptamat

Identifying flow defects in amorphous alloys using machine learning outlier detection methods

Liang Tian[a,*], Yue Fan[b], Lin Li[a,*], Normand Mousseau[c]

[a] Department of Metallurgical and Materials Engineering, University of Alabama, Tuscaloosa, AL 35404, United States
[b] Department of Mechanical Engineering, University of Michigan, Ann Arbor, MI 48109, United States
[c] Département de physique, Université de Montréal, C.P. 6128, succ. Centre-ville, Montréal (Québec), Canada

ARTICLE INFO

Article history:
Received 27 March 2020
Revised 18 May 2020
Accepted 18 May 2020

Keywords:
Amorphous
Flow defects
Shear transformation zone
Activation and relaxation technique
Machine learning

ABSTRACT

Shear transformation zones (STZs) are widely believed to be the fundamental flow defects that dictate the plastic deformation of amorphous alloys. However, it has been a long-term challenge to characterize STZs and their evolutions by experimental methods due to transient nature. Here we first introduced a consistent, automated, robust method to identify STZs by linear based machine learning outlier detection algorithms. We exemplify these algorithms to identify the atoms of STZs in Cu64Zr36 metallic glass system, and verify this data-driven model with a physical based model. It is revealed that the average STZ size slightly increases with decreasing cooling rate.

Metallic glasses (MGs) possess remarkably high strength due to their unique amorphous structure that is lack of crystalline defect dislocations carrying plastic deformation [1–7]. However, their practical application as structural materials has been limited by the nearly negligible tensile ductility due to severe strain localization in the form of shear banding [8–12]. How shear bands form is strongly dependent on the collective behaviors of the hypothetical flow defect shear transformation zones (STZs) in the MGs [2,13–16]. The activation of STZs has been shown to be directly related with the fast secondary beta relaxation process [15,17,18], which can be related to the structural heterogeneity and bonding state [19–21]. From the perspective of potential energy landscape, this beta relaxation can be identified as hopping events across subbasins within an inherent mega-basin [18,22,23]. However, in practice, the STZs are difficult to determine by experiments directly [24–28] due to its transient nature in the disordered structure, rendering it hard to form a diffraction pattern in a realistic timeframe. In the atomistic simulations, on the other hand, the identification of STZs from localized atomic rearrangement without a structural indicator, largely rely on taking the theoretical STZ model as a priori [29-31], resulting in significant variations induced by thermal or stress stimulations [32–34].

Machine-learning (ML) has become an emergent and powerful tool in material science to create accurate predictive material models quickly and automatically for the rational design of novel materials [35–37]. For example, ML models have been created to establish complex processing-properties relationship, predict the mechanical properties of metallic alloys, phase diagram, crystal structures, melting temperatures of binary inorganic compounds, the formation enthalpy of crystalline compounds, band gap energies of certain classes of crystals, develop interatomic potential and energy functional for accelerated materials simulation [35,38–40]. Due to the disordered structural nature and the non-equilibrium dynamics [41], the MGs represent a unique system for ML. Successful examples include building the relationship between composition and glass forming ability [38,42,43], and identifying the structural feature of flow defects; but limited studies have been focused on the fundamental dynamic features of the flow defects.

Here we introduce a novel method of adopting ML outlier detection algorithms to identify the atoms involved in STZs during many thermally-activated events. We exemplify this algorithm to identify the size of STZs in a model $Cu_{64}Zr_{36}$ MG system with various cooling rates, and verify the data-driven model with a previous physical based model. Furthermore, it is revealed that the average STZ size slightly increases with decreasing cooling rate. The advantages of this machine learning outlier detection approach are automated detection, consistent results, robustness to a wide range of training data of ART simulations that can be applied in many different systems of amorphous solids [44].

$Cu_{64}Zr_{36}$ metallic glass samples with three different cooling rates were prepared by LAMMPS molecular dynamics simulation

* Corresponding authors.
E-mail addresses: liangtianisu@gmail.com (L. Tian), lin.li@eng.ua.edu (L. Li).

https://doi.org/10.1016/j.scriptamat.2020.05.038
1359-6462/

software [45]. Specifically, the system was quenched from the equilibrium liquid state at 2000 K (equilibrated for 2 ns) to ~ 0 K, at three cooling rates of 10^{11} K/s, 10^{13} K/s and instant quenching, respectively, under Nose-Hoover thermostat and zero-pressure barostat. Further equilibration for 2 ns at near 0 K and minimization were applied to three quenched samples. Each sample contains 2000 atoms, located inside a simulation box with periodic boundary conditions in all three directions. The activation-relaxation technique (ART) was used to probe the local structural excitations of three samples, providing ~4000 transition events data connecting the initial, saddle and final states of STZs [46–49]. The details of ART are included in the supplemental materials. All post-processing tasks, including these machine learning outlier detection algorithms, are conducted by using self-developed open source software package ART_data_analyzer [44], which has been integrated into the ART-nouveau project in gitlab to facilitate the automation of running ART simulations and ART post-processing tasks in parallel.

In this study, we performed the correlation analysis between the atomic displacement and atomic level strains defined in reference [50] to identify the zone of atomic rearrangement (non-affine displacement) as the flow defect STZs. The physical insight is that the atoms going through inelastic deformation will deviate from a linear (pure elastic) strain-displacement relationship. Identifying the atoms of STZs essentially becomes obtaining a robust way to identify atoms that are outliers to the linear relation. The extent of deviation from a linear relation determined the magnitude of inelastic rearrangement. The atomic level von Mises shear strain η_i^{Mises} and volumetric strain η_i^{hydro} are defined as

$$V_i = \sum_{j\in N_i} d_{ji}^{0T} d_{ji}^{0}, W_i = \sum_{j\in N_i} d_{ji}^{0T} d_{ij}, J_i = V_i^{-1} W_I, \eta_i = \frac{1}{2}\left(J_i J_i^T - I\right) \quad (1a)$$

$$\eta_i^{hydro} = \frac{1}{3} Tr\eta_i \quad (1b)$$

$$\eta_i^{Mises} = \sqrt{\frac{1}{2} Tr(\eta - \eta_m I)^2} \quad (1c)$$

where d_{ji}^0 is the displacement vector from atom i pointing to atom j before deformation, d_{ji} is the displacement vector from atom i pointing to atom j after deformation. i is the index of atom of interest, j is the index enumerating over all neighboring atoms N_i. V_i, W_i, J_i, η_i in Eq (1a) are the 3 by 3 matrices associated with atom i.

Machine learning outlier detection algorithms are used to identify the atoms in shear transformation zone. First, the atomic strains and atomic displacement of all atoms for each of the processes of initial-saddle, saddle-final, initial-final are calculated by the ART_data_analyzer package [44]. Atomic strain and atomic displacement calculations by ART_data_analyzer have been verified by Ovito [51]. Second, linear regression based machine learning algorithms implemented in scikit-learn machine learning package [52], are adopted to correlate the atomic strains and atomic displacements of all 2000 atoms from the initial state to saddle state for all filtered events in each MD sample. According to the cooperative shear model, the activation volume is crucial to the ductility of the metallic glass [16,25]. It is worthwhile to mention that indirect experiments (e.g. nanoindentation) to measure the size of STZs usually characterize the state transition from initial state to final state, which usually involves larger amount of atoms than the atoms going through inelastic deformation during the activation stage [22,25,53]. Therefore, we focus on the activation stage of STZs (i.e., from initial to saddle states) on the transition path, so that the individual STZ features can be clearly identified by avoiding the potential autocatalytic process upon the relaxation stage from the saddle to final states [53].

Fig. 1 shows a schematic of how these machine learning algorithms (described in details in supplementary materials) can find the outlier atoms that go through inelastic rearrangement during the activation stage of an STZ event. The linear based machine learning outlier detection algorithms will be trained on the dotted train data to get the optimized model parameters. With a user-defined parameter called the *relative residual threshold*, inliers are determined as the atoms located within the dashed threshold boundary; while outliers are identified as those outside of dashed boundaries. The *relative residual threshold* parameter is defined as the ratio of the desired absolute error tolerance to maximum deviation in atomic von Mises shear strain. It is noteworthy that the regular linear regression model is trained on all the data (including both inliers and outliers) to minimize the least square cost function, which will result in a linear model that maximizes the probability of observing all training data rather than inlier data. The trained linear models will be inferior (for the purpose of outlier detection) to the linear model trained by only inlier training data, which can be automatically identified by robust linear model ML algorithms. Therefore, this ML approach is very robust to outliers, in terms of both eliminating the effect of outlier training data on the trained machine learning model parameters and maximizing the probability of successfully classifying any abnormal training data as outliers. In this study, the conventional cross validation procedure for verifying the model predictability is not necessary because the purpose of our ML algorithms is to successfully identify any outlier among all training data, instead of making an accurate prediction for all training data. Therefore, the performance of various ML algorithms will be judged based on how these algorithms are sensitive to identify the outlier training data, and how the identified outlier atoms can match the physically meaningful properties of STZ.

How the machine learning outlier detection algorithms identify the outlier atoms of each thermally activated event independently is shown in Fig. 2. The ML trained linear model of each event is trained by the LinearRANSAC algorithm independently. With a *relative residual threshold* parameter progressively increasing, the number of outlier atoms is progressively reduced. The convergence criteria are determined by a two consecutive critical slope stopping criteria. A common relative residual threshold parameter was used for all filtered events in the samples. This parameter is determined by conducting a parameter sweep on this relative residual threshold parameter with respect to the average number of found outlier atoms of all 4418 filtered events. Based on our comprehensive tests on critical slopes vs. relative residual threshold detailed in supplemental materials, 0.54 is chosen as the common relative residual threshold value for all the events. For the examples of three events in Fig. 2, the number of outlier atoms is 4, 6, 9 for each event from left to right. Moreover, we verify that all these outlier atoms identified by our data-driven method are indeed connected and move cooperatively in each thermally activated event, which works surprisingly well and further prove that the linear based ML algorithms can indeed capture the physics principle behind. In addition, this common critical residual threshold value allows all the events of the three samples to reach the very close level of convergence with respect to the average number of outlier atoms. The benefit of this data-driven ML outlier detection approach is that it is more robust to the outliers inside training data to use only inlier data to capture the underlying physics, without the need of making an assumption of a physical rule in advance.

In this study, we used three linear based ML models to identify outliers. The results are demonstrated in Fig. 3 by performing a parameter sweep of an average number of outlier atoms against the *relative residual threshold*. The optimum model that is most sensitive to outliers will predict the average number of outliers whose

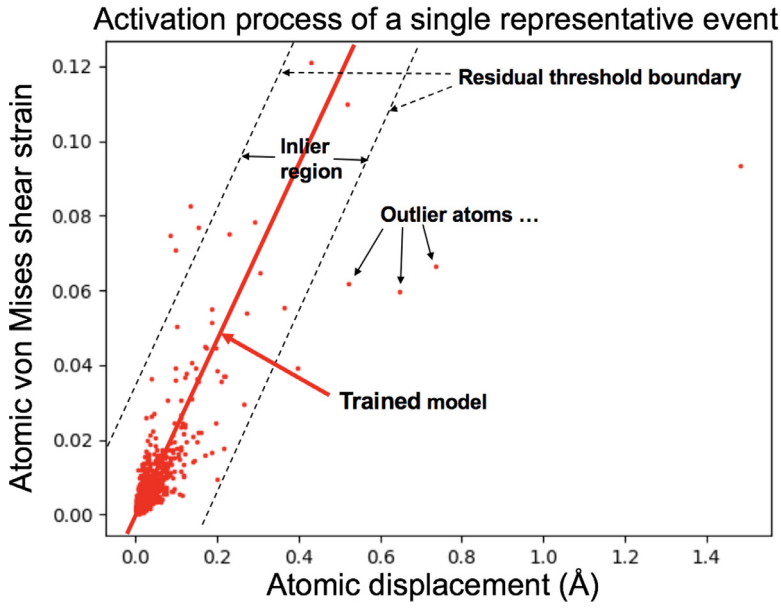

Fig. 1. A schematic showing the methodology to find the inelastically rearranged atoms during the activation process of a single STZ event by a machine learning outlier detection algorithm. The figure shows the relation between the atomic von Mises shear strain vs atomic displacement for all 2000 atoms in this event. Each red dot stands for a single atom. The red line stands for a machine learning model trained by these red dots (the model training process is demonstrated in supplementary materials). The black dashed line stands for the maximum error tolerance boundary between the predicted shear strain by the trained machine learning model and the actual shear strain. This maximum tolerance is controlled by a parameter called *the relative residual threshold*, which is the percentage of maximum deviation in shear strain and can be determined by a double slope convergence criterion. (For interpretation of the references to colour in this figure legend, the reader is referred to the web version of this article.)

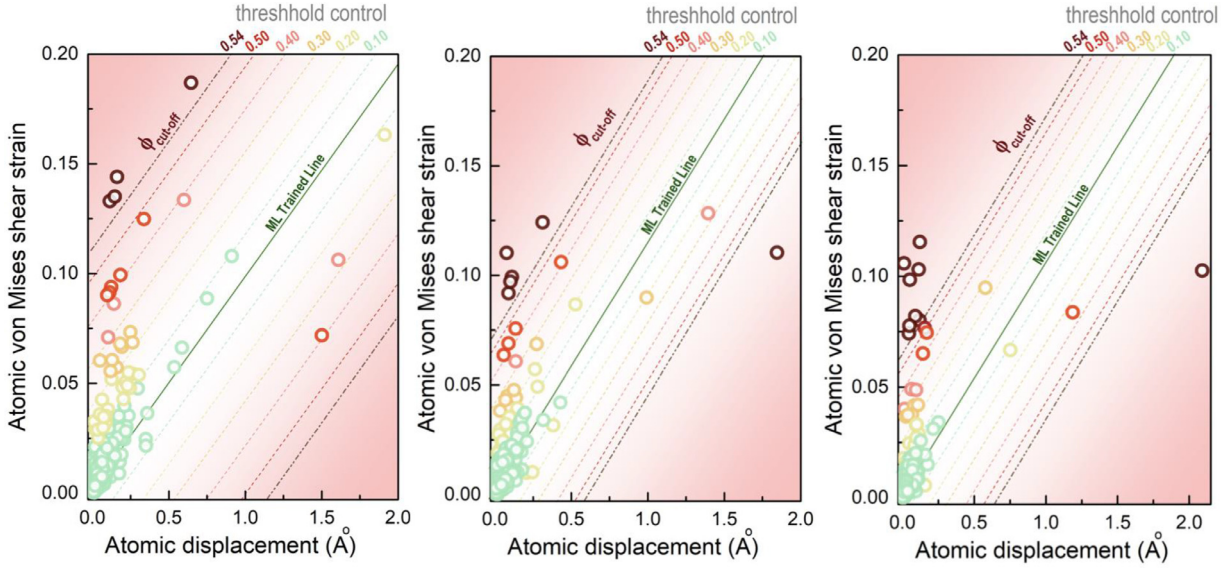

Fig. 2. The automation process of the LinearRANSAC machine learning algorithm identifies the outlier atoms of each individual thermally-activated event. (a)–(c) represent three representative independent events in a 10^{11} K/s cooling rate sample. All dash lines correspond to the residual threshold boundaries with color representing different relative residual threshold ϕ values (with $\phi_{cut-off}$ 0.54). The *relative residual threshold values* are 0.1, 0.2, 0.3, 0.4, 0.5, 0.54 from the most inner dash lines to the most outside dash lines.

value are most stable against the decreasing *relative residual threshold* (e.g. LinearRANSAC model in Fig. 3). Accordingly, the LinearRANSAC model is the most sensitive model in successfully classifying the correct inliers and outliers so that the average number of outlier atoms increase relatively slowly with decreasing relative residual threshold parameter.

Fig. 4 displays the averaged properties of identified outlier atoms constructing STZs for all filtered events in three samples when a common relative residual threshold value 0.54 is used in three above-mentioned linear based ML models. The average number of atoms in STZs during activation stage is around 4, which is close to the previous findings on a similar CuZr system based on a physical model [32]. This is consistent with the shear transformation zone region with a size of 4–6 atoms proposed by Argon [54]. Furthermore, all three models predict a consistent trend of increasing STZ atoms with decreasing cooling rate. Though not discerned by the physical model, this trend is physically plausible because with decreasing cooling rate, the sample tends to be more structurally relaxed and energetically stable with less free volume for atoms to rearrange so that the number of atoms associated with a shear transformation event should be increased [55,56].

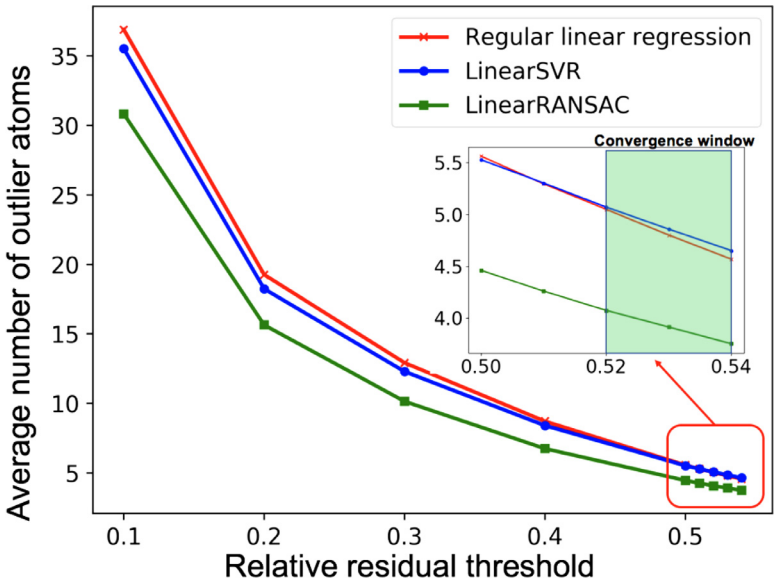

Fig. 3. Demonstration of using three linear based ML models to identify the outlier atoms in all thermally activated events of the 10^{11} K/s cooling rate sample. The critical relative residual threshold for identifying outlier atoms is chosen based on a double slope stopping convergence criterion. The critical slope double stopping criterion is that we stop the parameter sweep on the relative residual threshold when the two consecutive slopes of the curve (average number of outlier atoms vs relative residual threshold) are both smaller than a critical value, highlighted in the inset as convergence window. The reason to choose two consecutive slopes is to prevent the fluctuation of slope values for numerical calculation.

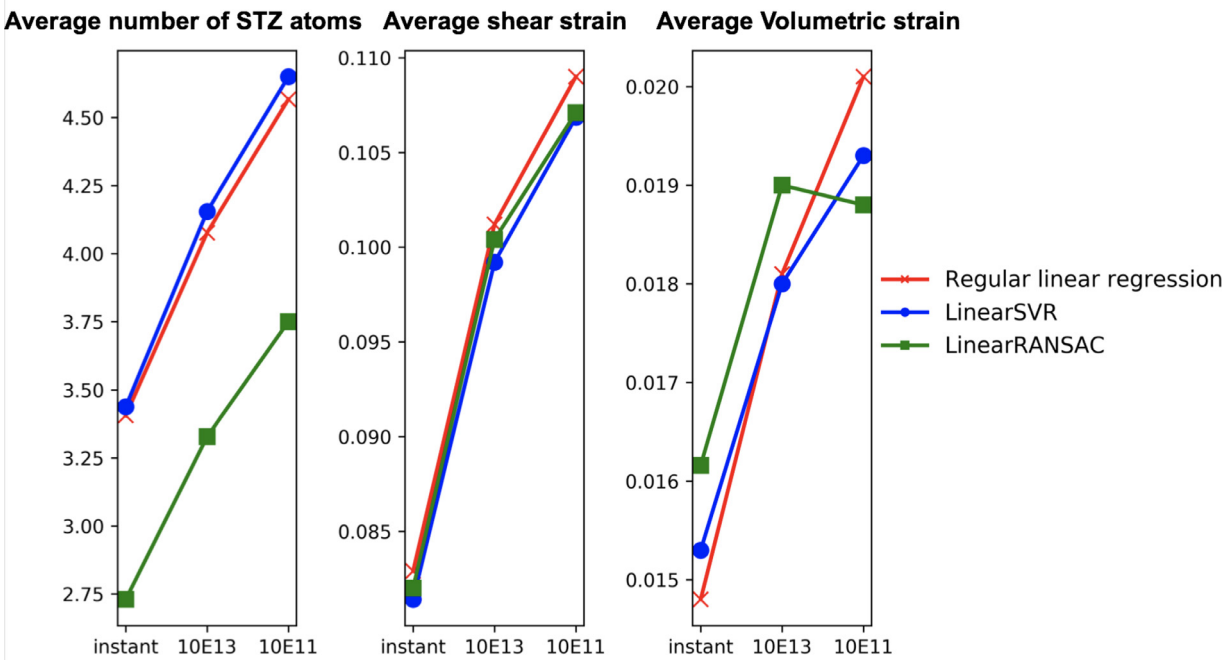

Fig. 4. The averaged properties of identified outlier atoms over all filtered events of three samples (cooling rates: instant quench, 10^{13} K/s, 10^{11} K/s), using relative residual threshold 0.54 for three linear based ML models. The averaged properties are calculated for the activation process (i.e., from initial state to saddle state).

The statistics of averaged properties (i.e. shear strain, volumetric strain) of identified outlier atoms using three linear based ML models, for all filtered events of three samples, are shown in Fig. 4. It is clear that the average shear strain during the activation process is around 0.1 for all three samples, closely matching the expected characteristic shear strain of an STZ usually on the order of 0.1 [1,57]. This 0.1 shear strain also aligns closely with the characteristic shear strain in shear transformation zone theory brought up by Argon [54]. As stated in Ref [1], the variation in shear strain quantity can definitely be related to the structural states of the glass under different thermal cooling rates.

Fig. 4 also suggested that the averaged volumetric strain of the outlier atoms in STZs is more than one order of magnitude less than that of shear strain, which further confirms that the nature of local atomic rearrangement is indeed the shear transformation in an STZ [16]. The ratio of averaged volumetric strain to averaged shear strain for three samples was calculated to be the order of 0.1, which aligns with shear transformation theory by Argon [54]. This suggests that the primary mode of deformation is shear deformation [16] instead of volumetric expansion/contraction during the activation process, which aligns with the Johnson-Samwer cooperative shear model [16,25]. We also calculated the cluster aver-

aged volumetric strain (dilatation) from initial to final process to be always positive for three samples, which indicates the creation of extra free volume during the activation of STZs. This extra free volume will allow the following activation of STZs to be much easier [58], consistent with the free volume theory and locally cooperative shear STZ theory [16,54].

In this study, we first demonstrated and developed a fundamentally distinct, novel, consistent, automated, robust computational method to identify the flow defect (STZ) in amorphous solids based on linear machine learning outlier detection algorithms, for resolving the long-term challenges of measuring STZs in experiments. LinearRANSAC is the most outlier-sensitive algorithm to accurately capture true STZ atoms, compared with LinearSVR and regular linear regression [44]. The average number of atoms in STZs during activation stage is very close to the results in literature [32] and also the number proposed by Argon [54]. The averaged shear strain and volumetric strain values during the activation stage also match the expected characteristic values of a STZ. The average number of STZ atoms is found not to be very sensitive to processing thermal cooling rates and tends to increase slightly with decreasing processing cooling rate. Based on the STZ dynamics theory [13], STZ size is one of the key input parameters that are needed to determine the rate of an STZ activation, linking elementary plastic events to mesoscopic and continuum plasticity. Therefore, materials with different activation rates of STZs could lead to a different cooperative deformation mode in response to thermomechanical loading, facilitating a rational design of metallic glass with enhanced ductility. This method is applicable to a wide range of different systems of amorphous solids and has already been implemented in our open source software ART_data_analyzer [44].

Declaration of Competing Interest

The authors declare that they have no known competing financial interests or personal relationships that could have appeared to influence the work reported in this paper.

Acknowledgements

LT and LL acknowledge the financial support by the U.S. Department of Energy, Office of Science, Basic Energy Sciences (BES), USA, by Award no. DE-SC0016164.

Supplementary materials

Supplementary material associated with this article can be found, in the online version, at doi:10.1016/j.scriptamat.2020.05.038.

References

[1] C.A. Schuh, T.C. Hufnagel, U. Ramamurty, Acta Mater. 55 (12) (2007) 4067–4109.
[2] T.C. Hufnagel, C.A. Schuh, M.L. Falk, Acta Mater. 109 (2016) 375–393.
[3] Y.Q. Cheng, E. Ma, Prog. Mater Sci. 56 (4) (2011) 379–473.
[4] W.H. Wang, Prog. Mater Sci. 52 (4) (2007) 540–596.
[5] T. Egami, Prog. Mater Sci. 56 (6) (2011) 637–653.
[6] J. Schroers, W.L. Johnson, Phys. Rev. Lett. 93 (25) (2004) 255506.
[7] D.B. Miracle, T. Egami, K.M. Flores, K.F. Kelton, MRS Bull. 32 (8) (2007) 629–634.
[8] A.L. Greer, Y.Q. Cheng, E. Ma, Mater. Sci. Eng. 74 (4) (2013) 71–132.
[9] Y.F. Gao, L. Wang, H. Bei, T.G. Nieh, Acta Mater. 59 (10) (2011) 4159–4167.
[10] L. Tian, L. Li, Int. J. Curr. Eng. Technol. 8 (2) (2018) 236–249.
[11] S. Khoddam, L. Tian, T. Sapanathan, P.D. Hodgson, A. Zarei-Hanzaki, Adv. Eng. Mater. 20 (9) (2018) 1800048.
[12] W. Chen, H. Zhou, Z. Liu, J. Ketkaew, N. Li, J. Yurko, N. Hutchinson, H. Gao, J. Schroers, Scr. Mater. 130 (2017) 152–156.
[13] E.R. Homer, C.A. Schuh, Acta Mater. 57 (9) (2009) 2823–2833.
[14] L. Li, N. Wang, F. Yan, Scr. Mater. 80 (2014) 25–28.
[15] Q. Wang, J.J. Liu, Y.F. Ye, T.T. Liu, S. Wang, C.T. Liu, J. Lu, Y. Yang, Mater. Today 20 (6) (2017) 293–300.
[16] W.L. Johnson, K. Samwer, Phys. Rev. Lett. 95 (19) (2005) 195501.
[17] T.J. Lei, L.R. DaCosta, M. Liu, W.H. Wang, Y.H. Sun, A.L. Greer, M. Atzmon, Acta Mater. 164 (2019) 165–170.
[18] H.B. Yu, W.H. Wang, H.Y. Bai, Y. Wu, M.W. Chen, Phys. Rev. B 81 (22) (2010) 220201.
[19] F. Moitzi, D. Şopu, D. Holec, D. Perera, N. Mousseau, J. Eckert, Acta Mater. 188 (2020) 273–281.
[20] D.P. Wang, J.C. Qiao, C.T. Liu, Mater. Res. Lett. 7 (8) (2019) 305–311.
[21] Y. Fan, T. Iwashita, T. Egami, Phys. Rev. E 89 (6) (2014) 062313.
[22] Y. Fan, T. Iwashita, T. Egami, Nat. Commun. 8 (1) (2017) 15417.
[23] C. Liu, P. Guan, Y. Fan, Acta Mater. 161 (2018) 295–301.
[24] I.-.C. Choi, Y. Zhao, B.-.G. Yoo, Y.-.J. Kim, J.-.Y. Suh, U. Ramamurty, J.-i. Jang, Scr. Mater. 66 (11) (2012) 923–926.
[25] D. Pan, A. Inoue, T. Sakurai, M.W. Chen, Proc. Nat. Acad. Sci. 105 (39) (2008) 14769.
[26] J.D. Ju, D. Jang, A. Nwankpa, M. Atzmon, J. Appl. Phys. 109 (5) (2011) 053522.
[27] C.A. Schuh, A.C. Lund, T.G. Nieh, Acta Mater. 52 (20) (2004) 5879–5891.
[28] H.-.B. Yu, W.-.H. Wang, K. Samwer, Mater. Today 16 (5) (2013) 183–191.
[29] J.S. Langer, Scr. Mater. 54 (3) (2006) 375–379.
[30] L. Li, E.R. Homer, C.A. Schuh, Acta Mater. 61 (9) (2013) 3347–3359.
[31] M. Zink, K. Samwer, W.L. Johnson, S.G. Mayr, Phys. Rev. B 73 (17) (2006) 172203.
[32] Y. Fan, T. Iwashita, T. Egami, Nat. Commun. 5 (2014) 5083.
[33] F. Delogu, Phys. Rev. Lett. 100 (25) (2008) 255901.
[34] D. Srolovitz, K. Maeda, V. Vitek, T. Egami, Philosoph. Mag. A 44 (4) (1981) 847–866.
[35] A.G.K. Tim Mueller, R. Ramprasad, Rev. Comput. Chem. (2016) 186–273.
[36] L. Ward, S.C. O'Keeffe, J. Stevick, G.R. Jelbert, M. Aykol, C. Wolverton, Acta Mater. 159 (2018) 102–111.
[37] J.M. Rickman, T. Lookman, S.V. Kalinin, Acta Mater. 168 (2019) 473–510.
[38] L. Ward, A. Agrawal, A. Choudhary, C. Wolverton, NPJ Comput. Mat. 2 (2016) 16028.
[39] D. Wei, J. Yang, M.-.Q. Jiang, B.-.C. Wei, Y.-.J. Wang, L.-.H. Dai, Phys. Rev. B 99 (1) (2019) 014115.
[40] Y.-.J. Hu, G. Zhao, M. Zhang, B. Bin, T. Del Rose, Q. Zhao, Q. Zu, Y. Chen, X. Sun, M. de Jong, L Qi, NPJ Comput. Mat. 6 (1) (2020) 25.
[41] F. Ren, L. Ward, T. Williams, K.J. Laws, C. Wolverton, J. Hattrick-Simpers, A. Mehta, Sci Adv 4 (4) (2018) eaaq1566.
[42] Y.T. Sun, H.Y. Bai, M.Z. Li, W.H. Wang, J. Phys. Chem. Lett. 8 (14) (2017) 3434–3439.
[43] A. Dasgupta, S.R. Broderick, C. Mack, B.U. Kota, R. Subramanian, S. Setlur, V. Govindaraju, K. Rajan, Sci. Rep. 9 (1) (2019) 357.
[44] L. Tian, L. Li, J. Ding, N. Mousseau, SoftwareX 9 (2019) 238–243.
[45] S. Plimpton, J. Comput. Phys. 117 (1) (1995) 1–19.
[46] N. Mousseau, L.K. Béland, P. Brommer, J.-.F. Joly, F. El-Mellouhi, E. Machado-Charry, M.-.C. Marinica, P. Pochet, J. Atom. Mol. Opt. Phys. (2012) (2012) 14.
[47] R. Malek, N. Mousseau, Phys. Rev. E 62 (6) (2000) 7723–7728.
[48] E. Machado-Charry, L.K. Beland, D. Caliste, L. Genovese, T. Deutsch, N. Mousseau, P. Pochet, J. Chem. Phys. 135 (3) (2011) 034102.
[49] G.T. Barkema, N. Mousseau, Phys. Rev. Lett. 77 (21) (1996) 4358–4361.
[50] J. Li, F. Shimizu, Least-square atomic strain, http://li.mit.edu/A/Graphics/A/annotate_atomic_strain/Doc/main.pdf, 2005.).
[51] S. Alexander, Modell. Simul. Mater. Sci. Eng. 18 (1) (2010) 015012.
[52] F. Pedregosa, G. Varoquaux, A. Gramfort, et al., J. Mach. Learn. Res. 12 (2011) 2825–2830.
[53] Y. Fan, T. Iwashita, T. Egami, Phys. Rev. Lett. 115 (4) (2015) 045501.
[54] A.S. Argon, Acta Metallurgica 27 (1) (1979) 47–58.
[55] C. Li, S. Kou, Y. Zhao, G. Liu, Y. Ding, Prog. Nat. Sci. 22 (1) (2012) 21–25.
[56] F. Zhu, S. Song, K.M. Reddy, A. Hirata, M. Chen, Nat. Commun. 9 (1) (2018) 3965 -3965.
[57] F. Boioli, T. Albaret, D. Rodney, Phys. Rev. E 95 (3) (2017) 033005.
[58] N. Wang, J. Ding, F. Yan, M. Asta, R.O. Ritchie, L. Li, NPJ Comput. Mat. 4 (1) (2018) 19.